

# Surface-Tension-Driven Flows of Coatings: Bondline Readout Formation

Richard H. J. Blunk\*\*—General Motors Corporation\*  
James O. Wilkes—The University of Michigan†

## INTRODUCTION

A uniform film thickness or filmbuild is desired to produce aesthetically appealing paint finishes. Small-scale paint-surface nonuniformities, such as orange peel, result in low distinctness of image (DOI) and gloss values, and, in turn, in poor coating appearances. The filmbuild must be high enough to enhance leveling and to protect the vehicle from corrosion and UV exposure, but low enough to reduce material costs and to prevent the film from sagging on vertical surfaces. Note that paint rheology is also an important factor affecting the leveling rate, and, in turn, the paint appearance; however, it is more difficult to adjust than filmbuilds in everyday automotive paint operations.

Today's automotive paint operations use different filmbuild specifications and/or paints with different flow characteristics for horizontal and vertical surfaces. For horizontal panels (e.g., hood, decklid, roof) the appearance specifications are more stringent since appearance attributes on these panels are more noticeable. As a result, higher filmbuilds and/or high-flow coating formulations are used to allow for better leveling, and, in turn, for smoother films, since gravity-driven paint-sagging effects are absent on horizontal panels. For vertical panels (e.g., fenders, doors, facias) the specifications are less stringent since filmbuild nonuniformities and defects are less noticeable on vertical panels. As a result, low filmbuilds and/or low-flow coatings are used on vertical panels to help prevent sagging, at the expense of producing less than superior finishes.

With the increased use of high-solids (and high-flow) clearcoats<sup>1</sup> and customer-driven desired increase in coating reflectivity and smoothness, a large number of coating defects caused by Marangoni-type<sup>2</sup> or surface-tension-driven flows have become increasingly more prevalent, especially when painting vehicles with horizontal body panels made from polymeric composites such as polyester-styrene based sheet molding compound (SMC). Unfortunately, these defects cannot be eliminated easily via

*Bondline readout (BLRO) is a coating defect frequently observed on adhesively bonded, polymeric automotive body panels. This paper addresses ridging BLRO in clearcoats, not optical and mechanical BLRO, which are characterized by metal-flake orientation (dark/light effects) in basecoats and by distortion in substrates, respectively. Ridging BLRO is due to film thickness differences and results from Marangoni-type, surface-tension-driven flows. In this study, the effects of several parameters on BLRO are investigated experimentally. These parameters include initial film thickness, heating rate, viscosity, solvent-to-resin surface-tension ratio, and solvent volatility. The experiments clearly demonstrate three modes of BLRO flow—formation, flow-out, and reformation—that result from competing surface-tension-gradient forces (temperature- versus concentration-induced). Experimental results are used to validate a proposed BLRO mechanism and, in subsequent work, a BLRO-predicting numerical code.*

filmbuild adjustments. One such defect is known as bondline readout (BLRO) and is one form of “telegraphing”—revealing structural features through the coated part after the coating has cured. BLRO results from surface-tension-gradient flow, which in turn results from temperature gradients generated on the SMC surface during convection heating/curing of the paint. An underlying adhesive bond acts as a heat sink and generates cooler temperatures on the SMC surface directly over the bonds. Since surface tension increases with decreasing temperature, coating material is drawn from the nonbond regions,

\*R & D Center, MD 480-102-000, 30500 Mound Rd, Warren, MI 48090-9055, email: rick.blunk@gm.com.

†Department of Chemical Engineering, Dow Building, Ann Arbor, MI 48109-2136, email: wilkes@umich.edu.

\*\*Author to whom correspondence should be directed.

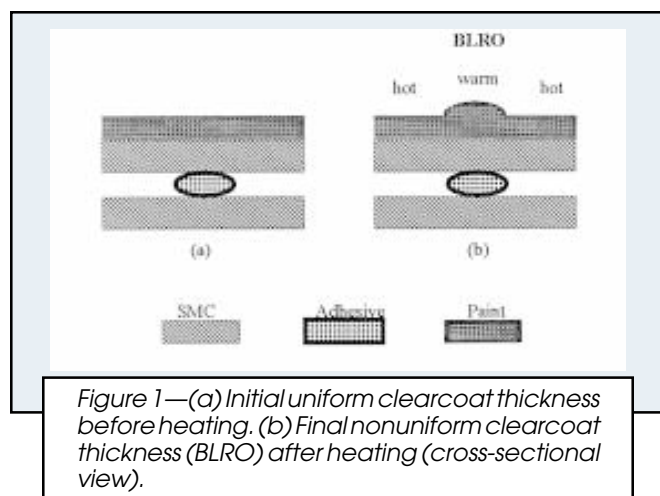


Figure 1—(a) Initial uniform clearcoat thickness before heating. (b) Final nonuniform clearcoat thickness (BLRO) after heating (cross-sectional view).

resulting in thicker films over the bonds. The end result is an undesirable outline or imprint in the coating surface of the underlying adhesive bond as shown in Figure 1. The bondline is, in effect, “readout” through the SMC panel and, subsequently, in the paint.

The coating defect (ridging BLRO) described previously and illustrated in Figure 1 is one of three types of BLRO observed on adhesively bonded, painted automotive parts. Ridging BLRO is due to film thickness variations produced from surface-tension-gradient flows and can occur in both clearcoats and basecoats, although clearcoat ridging is the topic of this paper. Ridging BLRO is the precursor to the second type of BLRO defect—optical BLRO—which occurs solely in basecoats. Optical BLRO is characterized by dark and light patterns (i.e., a color shift) near the bondline as a result of a different orientation of the metallic flakes in the high-flow bond area compared with the low-flow, nonbond area and/or a different packing density of the flakes between the thin and thick areas. In the third type of BLRO defect—mechanical BLRO—the SMC panel is deformed, due to the coefficient of thermal expansion difference and moduli difference between the SMC and adhesive, and the paint simply highlights or magnifies this deformation. Note that in the case of mechanical BLRO the paint film is of uniform thickness.

To eliminate the highly unacceptable BLRO, automotive manufacturers are forced to switch from polymeric to metallic body panels when using high-glamour/flow coatings, or from high-flow/high-glamour to low-flow/low-glamour coating systems when using polymeric body panels. Metal panels, of high thermal diffusivity, rarely produce significant temperature gradients and low-flow coatings are not as susceptible to surface-tension-gradient forces. Unfortunately, in most cases, these changes result in weight and cost penalties or inferior vehicle finishes.

The purpose of this experimental work is to obtain a better understanding of the mechanism of BLRO so that this clearcoat defect can be eliminated. Experimentally, the effects of several parameters on BLRO were studied, including initial film thickness, heating rate, viscosity, solvent volatility, and solvent-to-resin surface-tension ratio. Results of this work were used to develop and validate in subsequent work an efficient numerical code that predicts BLRO accurately.<sup>3</sup> This code can then be used to

investigate quantitatively the BLRO flow mechanism to provide information such as the magnitude of temperature- versus concentration-induced surface-tension gradients, the pressure and velocity distributions, and the relative magnitude of surface-tension, gravity, and viscosity effects, thereby reducing the number of costly and time-consuming experiments currently being performed.

### Proposed BLRO Mechanism

Figure 2 shows the BLRO film defect. Only half of the defect is illustrated due to symmetry. Four forces are involved in BLRO flow: (1) surface-tension gradient (driving force), (2) capillary pressure (leveling force), (3) viscosity (resisting force), and (4) gravity (leveling force). During the convection bake cycle, temperature variations exist across the film surfaces of adhesively-bonded SMC assemblies. These variations occur because the adhesive, having a higher thermal conductivity than air, acts as a heat sink, allowing heat conduction through the bond area. Material is then drawn towards the cooler bond area of high surface tension from the remoter areas. A nonuniform film build results and is frozen in at the onset of cure.

The degree of BLRO depends on competing flows—surface-tension-gradient flow increases BLRO while pressure-gradient flow decreases BLRO. The former, more commonly referred to as Marangoni flow, results from spatial temperature and/or concentration variations and because surface tension is temperature and concentration dependent. The resulting surface-tension gradient is equivalent to a shear stress driving-force. The latter, pressure-gradient flow, results from nonuniform film thicknesses caused by Marangoni flow. The pressures in the concave regions of the film (B and F) exceed that in the convex regions (A) due to surface-tension effects. Pressure differences also exist at similar locations along the bottom of the film due to gravity or hydrostatic effects, with pressures at C and E exceeding that at D. Surface-tension gradients cause flow from A to B, resulting in BLRO; gravity and surface tension, together with surface curvature, cause pressure-gradient flow from C and E to D, towards the thin convex regions, resulting in leveling. The degree of BLRO also depends on time.

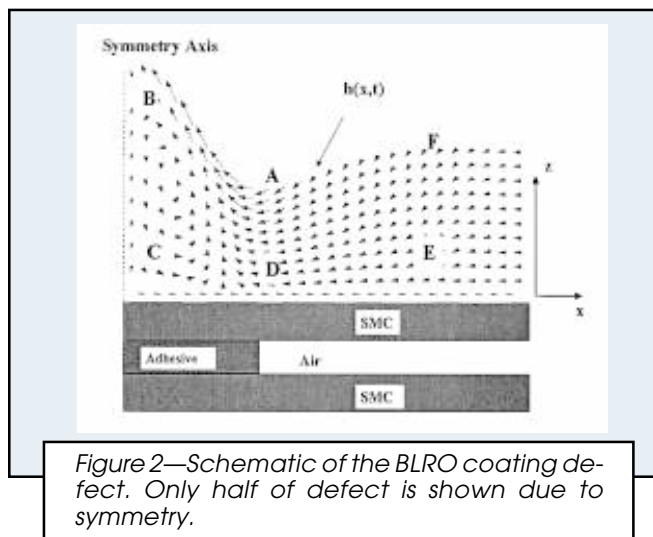


Figure 2—Schematic of the BLRO coating defect. Only half of defect is shown due to symmetry.

The velocity profiles through the film thickness for surface-tension-gradient and pressure-gradient flows are linear (Couette-like) and parabolic (Poiseuille-like), respectively. Depending on the relative magnitude of the two opposing flows, a circulation flow pattern can also be developed, which is shown near the symmetry line in *Figure 2*. This pattern was observed experimentally using fluorescence microscopy and by doping paint films with insoluble fluorescent dye particles. The combined velocity profile is given by:

$$u = \frac{\partial \sigma}{\partial x} \frac{z}{\mu} - \frac{\partial p}{\partial x} \frac{z}{\mu} \left( h - \frac{z}{2} \right) \quad (1)$$

where  $u$  is the  $x$ -component of velocity and  $\mu$  is the Newtonian viscosity.<sup>4</sup>

A mass balance shows that the time rate of change in film thickness  $h$  is:

$$\frac{\partial h}{\partial t} = -\frac{\partial J}{\partial x} \quad (2)$$

in which the flux  $J$  is obtained by integration of equation (1) over the film thickness ( $z = 0$  to  $h$ ):

$$J = \frac{\partial \sigma}{\partial x} \frac{h^2}{2\mu} - \frac{\partial p}{\partial x} \frac{h^3}{3\mu} \quad (3)$$

By substituting equation (3) into equation (2), the time evolution of film thickness becomes:

$$\frac{\partial h}{\partial t} = -\frac{\partial^2 \sigma}{\partial x^2} \frac{h^2}{2\mu} - \frac{\partial \sigma}{\partial x} \frac{\partial h}{\partial x} \frac{h}{\mu} + \frac{\partial^2 p}{\partial x^2} \frac{h^3}{3\mu} + \frac{\partial p}{\partial x} \frac{\partial h}{\partial x} \frac{h^2}{\mu} \quad (4)$$

Since the film is initially of uniform thickness and pressure, equation (4) indicates that BLRO or a nonuniform film thickness can only be generated when the surface-tension gradient is not constant (i.e., finite  $\partial^2 \sigma / \partial x^2$ ), which occurs if the temperature gradient varies with position. Moreover, to generate a symmetrical thickness profile similar to that shown in *Figure 2*, a symmetrical temperature profile is required; however, a linear (constant  $\partial T / \partial x$ ) and symmetrical temperature profile is physically unrealistic because the temperature gradient or heat flux at the symmetry line would be discontinuous.

Temperature and concentration variations affect viscosity and surface tension, which in turn affect BLRO flow. Surface-tension effects are most evident with the occurrence of three modes of BLRO flow—formation, flow-out, and reformation. The magnitude of the shear-stress-driving force (Levich-Aris boundary condition) is given by:

$$\tau = \nabla \sigma \cdot \bar{t} \equiv \frac{\partial \sigma}{\partial x} + \frac{\partial h}{\partial x} \frac{\partial \sigma}{\partial z} \equiv \left[ \left( \frac{\partial \sigma}{\partial T} \right) \left( \frac{\partial T}{\partial x} \right) \right] + \left[ \left( \frac{\partial \sigma}{\partial C} \right) \left( \frac{\partial C}{\partial x} \right) \right] \quad (5)$$

T-term                      C-term

where  $h$  is the film thickness,  $C$  is the solvent concentration,  $T$  is the temperature,  $\bar{t}$  is the unit vector tangent to the free surface, and  $x$  and  $z$  are coordinate directions. The surface-tension gradient is composed of two terms—the temperature-induced term (T-term) and the concentration-induced term (C-term). If the sum of the two terms is negative (positive), the shear stress acts in the negative

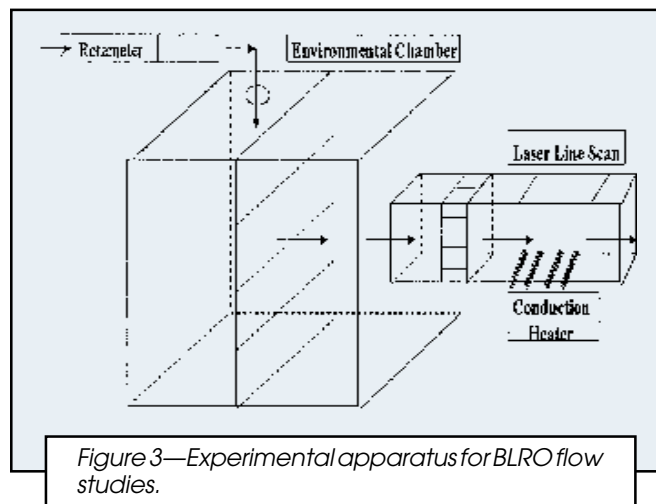


Figure 3—Experimental apparatus for BLRO flow studies.

(positive)  $x$ -direction. In equation (5), minus and plus signs are positioned directly over the partial derivatives. These signs are valid under all conditions used in this study. The signs for the temperature and concentration gradients are based on film conditions on the right-hand side of the symmetrical profile as presented in *Figure 2*. In the high-flow regions of interest, the temperatures near the symmetry line are always lower than those at larger  $x$ -values, i.e.,  $\partial T / \partial x$  is always positive. The sign of  $\partial \sigma / \partial T$  is always negative—surface tension decreases with increasing temperature. Thus, the T-term is always negative in this work and results in material flow towards the symmetry line (i.e., BLRO formation and reformation). Since the solvent concentration is always greater under the BLRO hump compared to that in thin regions, i.e.,  $\partial C / \partial x$  is always negative, due to solvent evaporation from a nonuniform thickness film, the sign of the C-term depends on the sign of its first partial derivative (unknown and delineated by a query “?”). If the solvent surface tension is less than that of the polymer resin, as is usually the case, then  $\partial \sigma / \partial C$  is negative and the C-term is positive. Also, if the magnitude of the C-term is greater than that of the T-term, material flows away from the symmetry line (i.e., flow-out or leveling). On the other hand, if  $\partial \sigma / \partial C$  is positive, the negative C-term augments the negative T-term and BLRO formation is enhanced. These temperature and concentration effects are demonstrated below.

## EXPERIMENTAL

*Figure 3* shows the apparatus, of which the major components are the conduction heater, which generates temperature gradients on its surface, and hence, surface-tension gradients in the coating; the environmental chamber, which provides a controlled setting for heat and mass transfer; and the non-contact, laser line-scan profilometer, which measures the time-varying, wet-film thickness profiles. Each component is described in detail elsewhere.<sup>3</sup> Work was done with an outside source (Analytical Measurement Technology, Madison Heights, MI) to develop the laser line-scan instrument in which the measurement mechanism is similar to that used in measuring the curvature of solid films for stress analyses.<sup>5</sup> Dr. Vardarajan Iyengar of the General Motors Research and Development

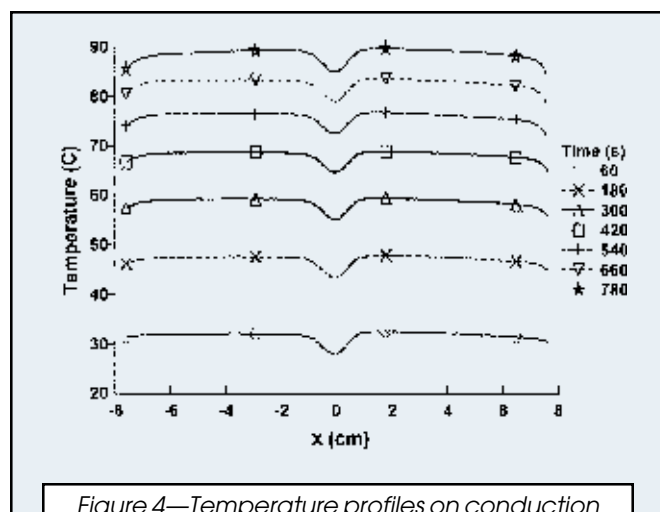


Figure 4—Temperature profiles on conduction heater surface 86 W.

Center and the principal author developed the calibration, measurement, and data analysis techniques needed to make the line-scan hardware operational. The air velocity in the environmental chamber was set at 26 cm/sec so that: (1) the air space above the heater was not saturated or partially saturated with the film solvent, (2) shear stresses on the wet film produced by air flow were insignificant compared to those produced by surface-tension effects, (3) Bénard cells would not form due to significant temperature gradients through the film thickness, and (4) boundary-layer theory for laminar flow past a flat plate could be used in subsequent numerical work to predict the external mass-transfer coefficient.<sup>6</sup> The conduction heater was constructed to produce a symmetrical temperature profile, thereby facilitating the subsequent numerical analysis, and, more importantly, enabling use of the laser line-scan profilometer, which scans in one direction only. The heater edges were well insulated with corkboard to reduce temperature-induced surface-tension gradient flow at the film edge or "picture-framing."<sup>2</sup>

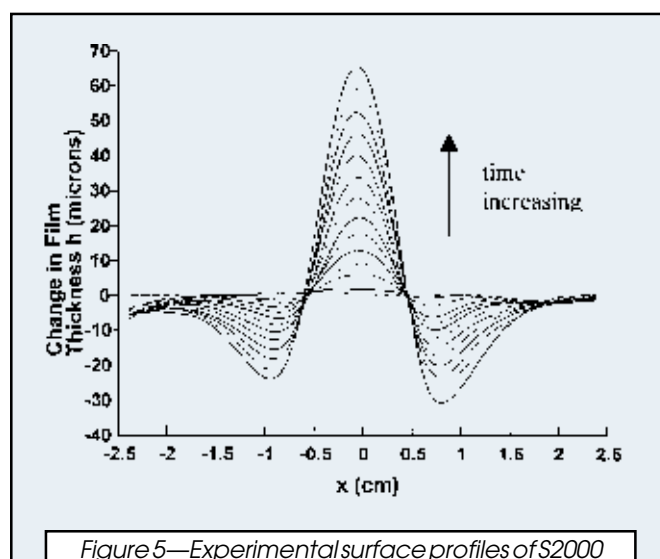


Figure 5—Experimental surface profiles of S2000 polybutylene film (178  $\mu$ m, 58 W).

Table 1—Polybutylene Resins Used in BLRO Flow Studies

Resin	Molecular Weight (wt. ave.)	Surface-Tension (dynes/cm) @ 20°C	Viscosity (Poise) @ 20°C
N1000 .....	1600	29.3	40
S2000 .....	1700	29.6	76
N4000 .....	3000	30.0	164

Table 2—Solvents Used in BLRO Flow Studies

Solvent	Boiling Point	Surface Tension (dynes/cm) @ 20°C
Decane .....	171	23.8
Undecane .....	196	24.7
Tridecane .....	234	25.5
1-Methylnaphthalene .....	242	38.0

BLRO flow experiments involve the following sequence:

- (1) calibrate the laser profilometer and level the heater using a biaxial clinometer (Applied Geomechanics, Model 900),
- (2) apply a thin film of coating to the surface of the conduction heater, covering a 10.2 cm  $\times$  12.7 cm area at a predetermined thickness, using a doctor blade (12.7 cm  $\times$  12.7 cm Gardco 8-Path Wet-Film Applicator),
- (3) cover the wet film with a 12 cm  $\times$  15 cm glass frame, with a 0.6 cm film-to-glass clearance, to eliminate dirt/dust contamination and solvent evaporation during film leveling,
- (4) allow the film to level for approximately 20 min,
- (5) remove the glass frame and quickly measure the initial film thickness in a non-scan area using a wet film thickness gage (Gardco, Model 154),
- (6) adjust the air flow with the rotameter (Omega, FL-401A),
- (7) turn on the heater and the laser profilometer simultaneously, and
- (8) record the current and the voltage readings from the ammeter (Data Precision 2480 with Fluke 80I-600 Current Probe) and the voltmeter (Hewlett Packard 3468A/B Multimeter).

The laser profilometer then scans the surface of the flowing film, collects slope data every 23 sec, and integrates these data to obtain surface profiles. Each experiment lasts either 690 sec (solvent-free coating) or 782 sec (solvent-filled coating). Reproducible heating of the conduction heater is achieved by performing a maximum of one experiment per day, which allows sufficient time for the conduction heater to cool down and reach thermal equilibrium. Reproducibility was confirmed by measuring the surface temperature of the heater with an IR imaging radiometer (Inframetrics, Model 760).

## Materials

An attempt was not made to simulate current and complex automotive clearcoat formulations and convective oven-heating processes. Instead, simple material and heat-

ing processes were chosen. A nonreacting, single-solvent polymer solution was used and heated via conduction, thus simplifying the study immensely while enabling the previous parameter effects to be investigated well. The coating materials must clearly demonstrate the effects of temperature and concentration on BLRO flow and, for some materials, should generate all three observed modes of BLRO flow—formation, flow-out, and reformation. Note that the crosslinking reaction was not studied here, even though it has an extremely large effect on BLRO. Crosslinking affects coating viscosity directly, through the formation of a three-dimensional structure, and affects surface tension indirectly, through a decrease in solvent diffusion to the surface. Nevertheless, the BLRO mechanism and the BLRO parameter effects can be investigated advantageously and the numerical code can be developed well without complicating matters by including curing effects, which can be incorporated into the code for future work.

The BLRO flow studies were conducted using solvent-free (100% resin) films and solvent-filled (14% by volume) films. Resin and physical property information are presented in *Table 1*. Cannon viscosity standards were chosen because the temperature dependence of their viscosities is well documented. Three polybutylene resins, of different viscosities, were selected to demonstrate the effect of viscosity on BLRO. Resin viscosity at 20°C approximately doubles each step in going from N1000 to S2000 to N4000. These resins had low surface energies, which promoted good wetting and spreading on the higher-energy glass surface, and low molecular weights, which enhanced the dissolution of these nonpolar resins into polar solvents. The low molecular weight also significantly influenced the mechanism of solvent evaporation from solution, causing surface-controlled in favor of diffusion-controlled evaporation, and which fortuitously simplified subsequent numerical modeling efforts.<sup>3</sup>

The solvents used in this study are shown in *Table 2*. They were used with the N1000 and N4000 resins. Low-volatility solvents were selected to reduce the likelihood of Bénard cell formation. The solvent boiling points at 1 atm are considerably greater than 90°C—the maximum film temperature obtained in this work. The three nonpolar

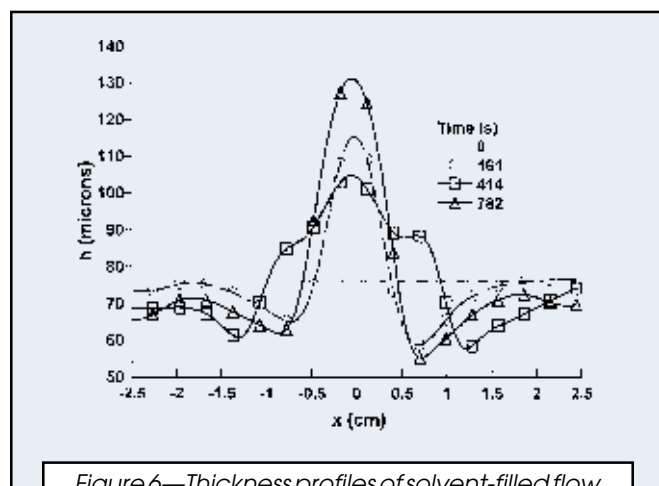


Figure 6—Thickness profiles of solvent-filled flow experiment (Undecane/N1000, 76  $\mu\text{m}$ , 86 W).

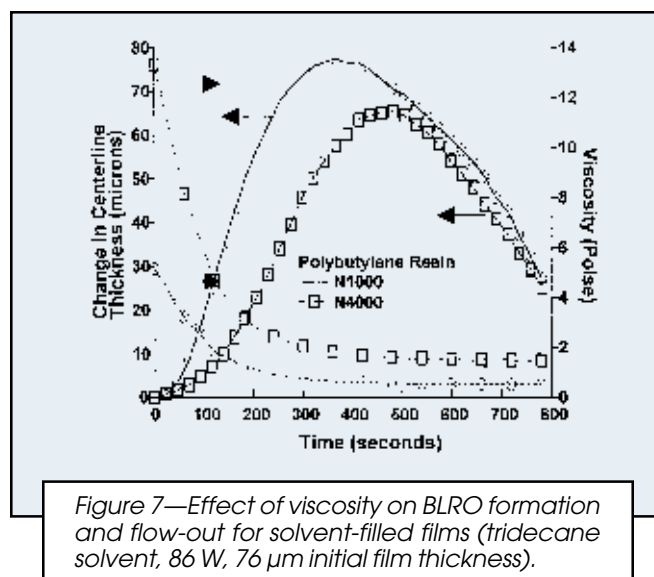


Figure 7—Effect of viscosity on BLRO formation and flow-out for solvent-filled films (tridecane solvent, 86 W, 76  $\mu\text{m}$  initial film thickness).

solvents (decane, undecane, and tridecane), of different volatilities and of nearly the same surface energies, were used to demonstrate the effect of volatility. Tridecane and 1-methylnaphthalene solvents, which have different surface energies and nearly the same volatility, were used to demonstrate the solvent-to-resin surface-tension ratio effects.

## RESULTS AND DISCUSSION

### Experimental Heat Transfer

The temperature profiles in the  $x$ -direction of the conduction heater surface were measured using an IR radiometer (Inframetrics, Model 760) and are shown in *Figure 4*. Data were collected at 60-sec intervals up to 780 sec. Data are shown at 120-sec intervals. The Inframetrics outline software was used to analyze temperatures centered on the heater surface, extending 7.62 cm in the  $x$ -direction (340 pixels) and 1.0 cm in the  $y$ -direction (50 pixels). The conduction heater was heated at a high heating rate of 86 W. Additional heat-transfer experiments were done using lower heating rates of 39 and 58 W. Steady-state conditions were never realized because surface temperatures continued to increase after 780 sec.

### BLRO Flow Studies

Again, two types of flow experiments were performed, using solvent-free films and using solvent-filled films. Profile results from two BLRO flow experiments, representing the two general types of experiments, are discussed later.

### Solvent-Free BLRO Flow Experiment

Typical surface profiles are shown in *Figure 5*. S2000 polybutylene, a medium heating rate of 58 W, and an initial film thickness of 178  $\mu\text{m}$  were used. Slope measurements were made every 23 sec for 690 sec. Only half of the profiles are shown for clarity. The laser scanned the centerline region and traveled  $\pm 2.38$  cm in the  $x$ -direction.

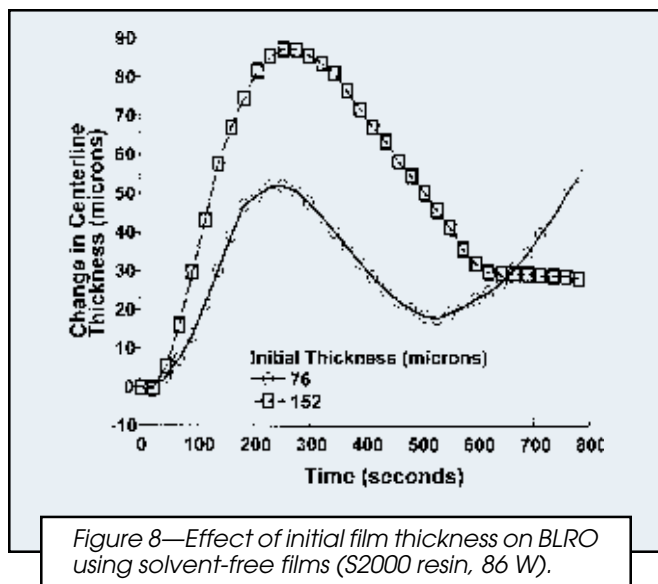


Figure 8—Effect of initial film thickness on BLRO using solvent-free films (S2000 resin, 86 W).

The following observations and speculations were made:

(1) BLRO is generated from temperature variations on the conduction heater surface. Material in the cooler centerline region of high surface tension draws material in from the warmer regions of low surface tension.

(2) BLRO continues to increase with time throughout the 690-sec flow experiment because the temperature-gradient driving-force increases slightly with time and the film viscosity decreases with time.

(3) The surface profile is not quite symmetric. The valley on the right-hand side of the centerline is greater than that on the left-hand side, which results from a nonsymmetric temperature profile similar to that shown in Figure 4.

(4) Area is conserved. The combined area of the two valleys is equal to the area of the BLRO hump.

(5) The change in film thickness is plotted in Figure 5, not the actual film thickness. The laser profilometer measures surface profiles, not thickness profiles. Thickness

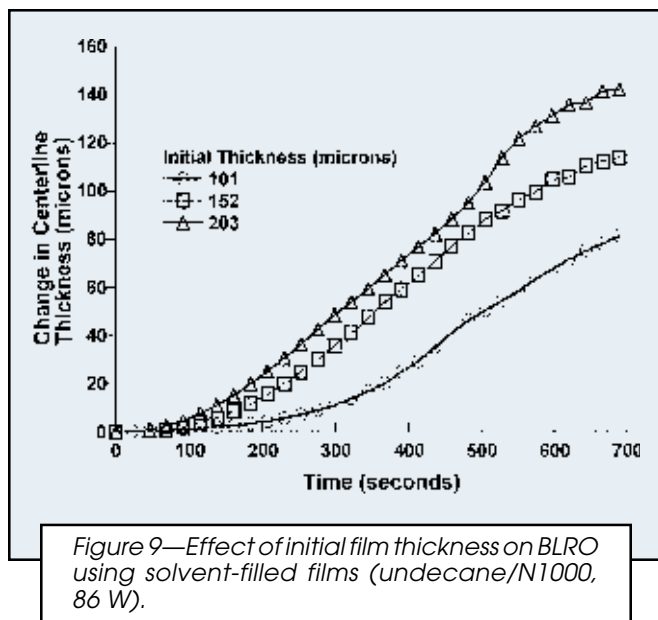


Figure 9—Effect of initial film thickness on BLRO using solvent-filled films (undecane/N1000, 86 W).

profiles are obtained by adding the initial film thickness to the surface profiles.

(6) The changes in film thicknesses at  $x = \pm 2.38$  cm are not identically zero, because the flow experiments did not conserve mass completely within the scan region and numerical leveling, used to eliminate tilt, forces the resulting profiles to conserve mass by shifting the zero-line slightly.<sup>3</sup>

### Solvent-Filled BLRO Flow Experiment

Figure 6 shows representative thickness profiles using an undecane/N1000 polymer solution with an initial solvent concentration of 14% (vol), a high heating rate of 86 W, and an initial film thickness of 76  $\mu\text{m}$ . Slope measurements for solvent systems were made with the line scan every 23 sec for 782 sec. Although symmetry was rather good, these worst-case experimental conditions resulted in the largest amount of profile nonsymmetry observed in this study. These experimental conditions also resulted in the formation of all three modes of BLRO flow—formation, flow-out, and reformation.

The following observations and speculations were made:

(1) At approximately 161 sec, i.e., during BLRO formation, flow again results mainly from temperature-induced, surface-tension gradients. Concentration-induced, surface-tension gradients are assumed small at these early times because BLRO flow-out or broadening of the BLRO hump is not apparent.

(2) At approximately 414 sec, i.e., during BLRO flow-out, leveling is obvious as the BLRO hump broadens and decreases in height. The valleys also appear to flow away from the centerline region. During flow-out, concentration effects dominate. Solvent-concentration variations are significant along the film surface and result from nonuniform solvent evaporation, and from nonuniform film thicknesses generated during BLRO formation. The percentage decrease in solvent concentration in the thinner valley region is larger than that in the thicker film regions (e.g., centerline region). This same effect was observed by Marangoni in the "Tears of Strong Wine" study.<sup>7</sup> The thicker regions, having a large solvent reservoir, became more solvent-concentrated than the thinner valley regions, having a small solvent reservoir. Since the surface tension of the undecane solvent is less than that of the N1000 resin, the surface tension in the low-solvent valley regions exceeds that in the high-solvent thicker regions. As a result, material fills in the valleys from the thicker, lower surface-tension regions, which in turn decreases the BLRO hump and creates a valley further away from the centerline.

(3) At approximately 782 sec, i.e., during BLRO reformation, the BLRO hump height increases and its width decreases, and new valleys form near the centerline region. BLRO reformation occurs because temperature effects again dominate. Temperature gradients increase slightly with time while the large concentration gradients, formed during the latter stages of formation and the early stages of flow-out, decrease with time as solvent film concentrations approach zero.

### BLRO Parameter Study

**VISCOSITY EFFECTS:** Viscosities, as functions of temperature and solvent concentration, were measured with a controlled strain-rate rheometer (Haake M10) using a cup-and-bob sensor geometry. The viscosities were constant in the strain-rate range up to approximately  $500 \text{ sec}^{-1}$ . Thus, the materials used in this work were considered Newtonian. No elastic effects or yield stresses were anticipated or observed.

The effect of viscosity on BLRO flow for solvent-filled films is shown in *Figure 7*. Tridecane/N1000 and tridecane/N4000 films (86 W and 76  $\mu\text{m}$  initial thickness) were tested. The change in centerline film thickness, not the entire thickness profile, is plotted against time and represents the degree of BLRO. The corresponding centerline resin viscosities are also plotted against time. Note that these viscosities are based on the initial 14% by volume solvent concentration. The effects of solvent loss on viscosity are not shown here. BLRO formation and flow-out are observed. The latter occurred because the tridecane has a lower surface tension than the resins, and as solvent concentration gradients are produced, opposing concentration-induced surface-tension gradients outweigh those induced thermally. *Figure 7* shows that the rate of BLRO formation is greater for the lower viscosity film (tridecane/N1000) than the higher viscosity film (tridecane/N4000), as expected. Also, the onset time for flow-out is less for the lower viscosity film (368 sec) than for the higher viscosity film (483 sec), suggesting that the spatial solvent concentration gradients were developed sooner for the lower viscosity film. This concentration-gradient development seems reasonable since the thickness differences during BLRO formation between the centerline and valley regions, which generate the concentration gradients, were greater for the lower viscosity film.

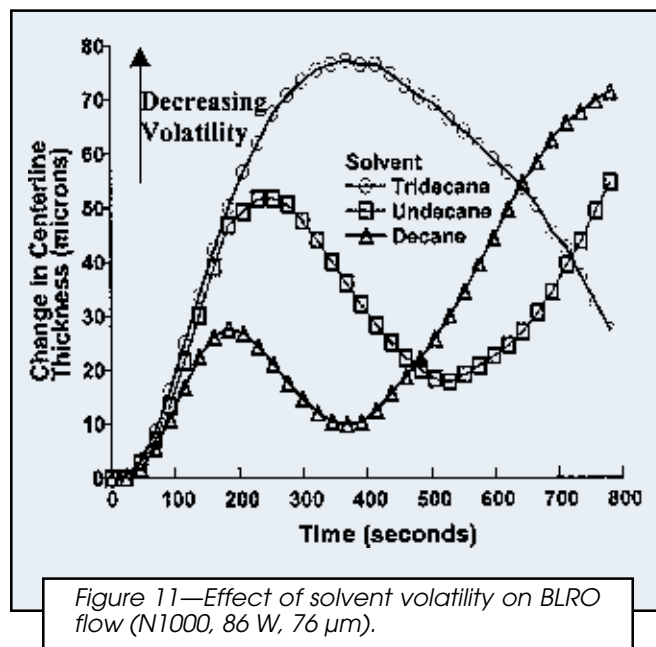
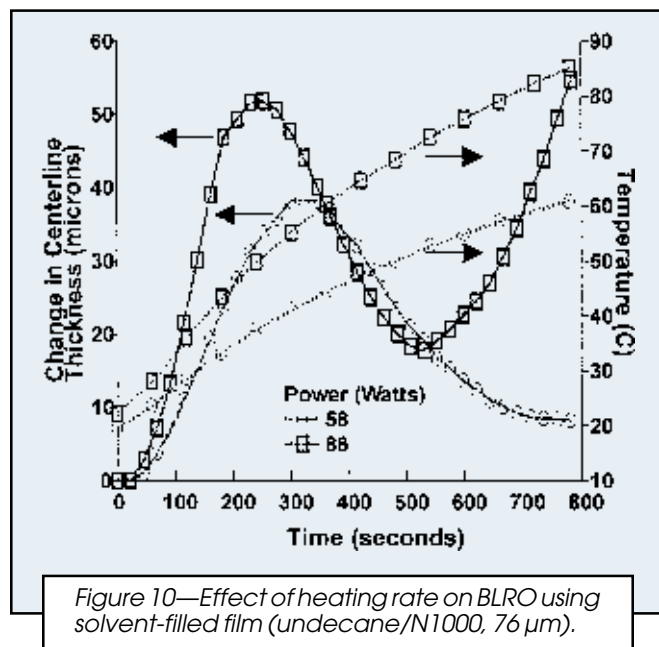
**INITIAL FILM-THICKNESS EFFECTS:** The degree of BLRO depends on competing flows: surface-tension-gradient flow increases BLRO while pressure-gradient flow decreases

BLRO. Since surface-tension-driven and pressure-driven flow rates are proportional to the thickness squared and cubed, respectively, surface-tension effects are expected to predominate for thin films, resulting in a large degree of BLRO; whereas, pressure-leveling effects are expected to predominate for thick films, resulting in a small degree of BLRO.

*Figure 8* presents results from experiments investigating the effects of the initial film thickness on BLRO. The S2000 polybutylene resin, heated at 86 W, was applied on the heater surface at three different film thicknesses—101  $\mu\text{m}$ , 152  $\mu\text{m}$ , and 203  $\mu\text{m}$ . Again, the change in centerline thickness is plotted against time. The degree of BLRO increased with increasing initial film thickness, suggesting that the surface-tension effect was predominant in the thickness range used. Subsequent work presents numerical results demonstrating conditions where pressure-leveling effects are predominant. Nevertheless, leveling effects are present in *Figure 8*. At a particular time, a reduction in the rate of BLRO increase was observed, going from a low- to high-film thickness curve (increments of 51  $\mu\text{m}$ ).

The film temperatures in all three experiments were essentially equivalent and equal to the heater surface temperatures (small thermal Biot number).<sup>8</sup> It is possible, however, that the film temperatures were not quite identical due to convective heat transfer. Heat convection is more apparent in thick films (high film velocities) than in thin films (low film velocities). The effect of heat convection on BLRO is discussed in detail elsewhere.<sup>3</sup>

Initial film-thickness effects from two solvent-filled experiments are shown in *Figure 9*. Undecane/N1000 films were heated at 86 W with initial film thicknesses of 76  $\mu\text{m}$  and 152  $\mu\text{m}$ . The change in centerline film thickness is plotted against time. With solvent-filled films, the initial film thickness not only affects the competing surface-tension and pressure-leveling flows, but also affects the magnitude and direction of the surface-tension-induced shear stresses indirectly. Details of numerical work conducted by the principal author on the effect of the transport phe-



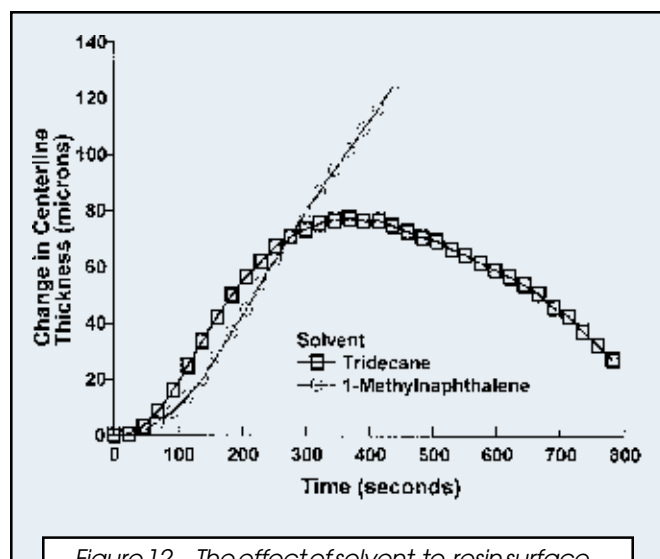


Figure 12—The effect of solvent-to-resin surface-tension ratio on BLRO (N1000, 86 W, 76  $\mu\text{m}$ ).

nomena on BLRO are discussed elsewhere.<sup>3</sup> For the experimental conditions used here, solvent convection affects BLRO significantly more than does thermal convection.

As shown in Figure 9, the initial film thickness affects BLRO significantly. During BLRO formation, for times less than 273 sec, the thick film generated more BLRO than the thin film due to dominant surface-tension-gradient flow. With a nearly identical shear-stress distribution applied to the surface of the thin and thick films, the no-slip condition at the glass surface prevented the thin film from generating large flow rates. The initial film thickness also affected the BLRO flow-out and reformation modes by altering the solvent concentration gradients along the film surface. The data show that the concentration gradients developed and disappeared more rapidly with the thinner film. The BLRO flow-out onset times were about the same for the two curves, even though the thicker film was expected to have lower onset times based on its larger centerline-to-valley thickness. Also, BLRO reformation was observed with the 76  $\mu\text{m}$  film and not with the 152  $\mu\text{m}$  film. The solvent concentration was reduced more rapidly with thin films than with thick films, for the same amount of solvent loss, because the former has a smaller solvent reservoir.

**HEATING RATE EFFECTS:** Figure 10 presents results from the heating-rate parameter study. The undecane/N1000 solvent-filled film was applied at an initial thickness of 76  $\mu\text{m}$  and heated at power levels of 58 W and 86 W, which correspond to average heating rates of 0.05°C/sec and 0.08°C/sec, respectively. The centerline-thickness change and the centerline surface temperature of the conduction heater are plotted against time. These temperatures were obtained experimentally. Heating rate affects BLRO significantly. Thickness results indicate that temperature gradients along the film surface are established more rapidly with increasing heating rate. During BLRO formation, at times less than 200 sec, BLRO was greater for the higher-power curve. Viscosity effects must also be considered since lower viscosities were generated at the

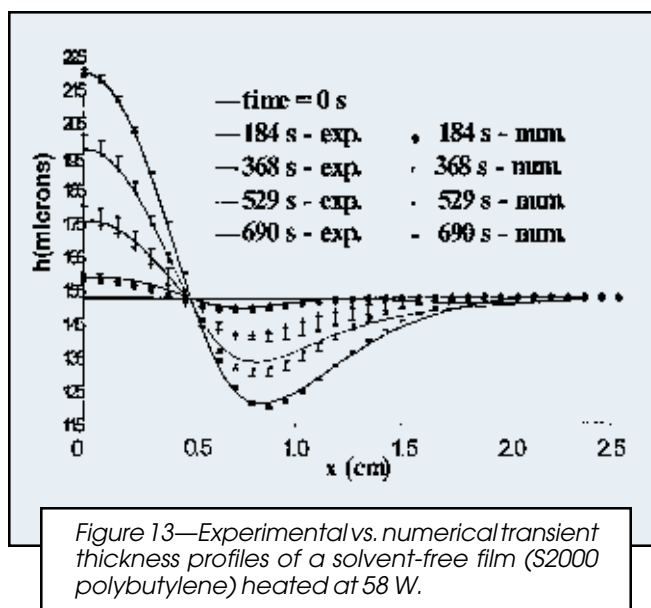


Figure 13—Experimental vs. numerical transient thickness profiles of a solvent-free film (S2000 polybutylene) heated at 58 W.

higher-power setting, due to higher temperatures, resulting in an increase in surface-tension flow.

Thickness results also indicate that surface concentration gradients change more rapidly with increasing heating rate. Because the centerline-to-valley thicknesses, generated during BLRO formation, were greater for the higher power setting, concentration gradients were also greater. Consequently, as seen from Figure 10, flow-out occurred sooner at 86 W (276 sec) than at 58 W (345 sec), and the rate of flow-out was greater at 86 W. This difference in the rate of flow-out between the two power levels may also have resulted from an increase in flow rate due to the higher film temperatures and lower film viscosities obtained with the higher heating rate. Heating-rate effects on surface concentration gradients were more apparent during the latter stages of BLRO flow, where reformation occurred at 86 W, but not at 58 W, showing that the solvent concentration gradients established during flow-out were reduced more rapidly at the higher heating rate as solvent concentrations were reduced significantly.

**SOLVENT VOLATILITY EFFECTS:** Solvent volatility effects on BLRO are displayed in Figure 11. The film consisted of the N1000 polybutylene resin dissolved in a single solvent, with an initial solvent concentration of 14% by volume. Three solvents of different volatilities were used. The tridecane, undecane, and decane solvent boiling points at 1 atm are 234°C, 196°C, and 171°C, respectively. Since the evaporation mechanism is surface-controlled,<sup>3</sup> the solvent evaporation rate is inversely proportional to the boiling point. The three experiments were conducted using a high heating rate of 86 W and a 76  $\mu\text{m}$  initial film thickness.

Solvent volatility had a large effect on BLRO. Transition from one BLRO flow mode—formation, flow-out, reformation—to another was accelerated with increasing solvent volatility. The flow-out onset times for the tridecane, undecane, and decane films were 391, 276, and 207 sec, respectively. The reformation onset times for undecane and decane films were 552 and 391 sec, respectively. The experiment was not run long enough for reformation to

occur for the tridecane film. These onset times show that the rate of change of concentration gradients increased with increasing volatility. As solvent volatility increased, concentration gradients formed more rapidly during the latter stages of formation to generate early flow-out and disappeared more rapidly during the latter stages of flow-out to generate early reformation.

The rate of change of concentration gradients was controlled more by the solvent volatility than by the nonuniform thickness magnitude.

**SOLVENT-TO-RESIN SURFACE-TENSION-RATIO EFFECTS:** It was proposed that BLRO flow-out can occur if  $\partial \sigma / \partial C$  in the shear-stress equation (equation 5) is sufficiently negative so that the resulting positive  $C$ -term dominates over the negative  $T$ -term, driving material away from the centerline. To check the above argument, experiments were performed using both negative and positive values for  $\partial \sigma / \partial C$ . Note that the sign of this derivative depends on the relative magnitude of surface-tension between the solvent and the resin; and hence, denotes the "solvent-to-resin surface-tension ratio."

In the first experiment, N1000 polybutylene resin was dissolved in a higher surface-energy, 1-methylnaphthalene solvent, which corresponds to a positive surface-tension ratio and a negative  $C$ -term. In the second experiment, the same resin was dissolved in a lower surface-energy, tridecane solvent, which produces a negative ratio and a positive  $C$ -term. Both experiments were run using a high heating rate of 86 W and a 76  $\mu\text{m}$  initial film thickness.

The changes in centerline thicknesses are shown in Figure 12. As expected, the 1-methylnaphthalene/N1000 film did not flow out. The BLRO hump continued to increase until at approximately 423 sec the slopes exceeded the upper limit of the laser profilometer ( $\approx 3.5^\circ$ ). Flow-out was not observed during the entire experiment. The shear stress, in the negative direction, was augmented by the negative  $C$ -term. In contrast, the tridecane/N1000 film did flow out. When the magnitude of the positive  $C$ -term exceeded the magnitude of the  $T$ -term at approximately 345 sec, material was driven away from the centerline region.

### Numerical Work

The experimental results agree qualitatively with those predicted based on the proposed BLRO mechanism. In addition, in subsequent numerical work, the proposed mechanism was confirmed quantitatively using the lubrication approximation method to derive the fourth-order partial differential Reynold's equation for the time dependence of film thickness.<sup>3</sup>

Figure 13 presents numerical and experimental profile results of an S2000 polybutylene film. The film with a measured initial thickness of 152  $\mu\text{m}$  was heated using a medium heating rate (58 W). Very good agreement is observed between the experimental and numerical profiles. One-sided error bars are displayed at each numerical datum point to illustrate the significance of a 25  $\mu\text{m}$  underestimation in measuring the initial film thickness. In this experiment, the initial thickness was measured to be 152  $\mu\text{m}$  using a wet-film thickness gage (Gardco, Model

154). The actual thickness could range anywhere from 152  $\mu\text{m}$  to 177  $\mu\text{m}$  because the probe lengths on the thickness gage were in 25  $\mu\text{m}$  increments. The numerical code was run twice using a 152  $\mu\text{m}$  and 177  $\mu\text{m}$  initial film thickness and the resulting thicknesses from the latter analysis were then reduced by 25  $\mu\text{m}$  so that these measurement error effects could be investigated. The small error bars shown in the figure show that the 25  $\mu\text{m}$  underestimation in initial thickness is insignificant. In addition, the error bars suggest that the actual initial film thickness was probably closer to 152  $\mu\text{m}$  than to 177  $\mu\text{m}$ .

### CONCLUSION

The experiments clearly demonstrated the effects of temperature and concentration on BLRO flow. Moreover, for certain experimental conditions, all three modes of BLRO flow—formation, flow-out, reformation—were generated, which provided qualitative information regarding the relative magnitudes of temperature-induced and concentration-induced surface-tension gradients. The experiments also clearly demonstrated the effects on BLRO flow of five parameters—viscosity, initial film thickness, heating rate, solvent volatility, solvent-to-resin surface-tension ratio.

Results from the BLRO flow experiments agree qualitatively with those anticipated from the proposed BLRO flow mechanism. The greatest asset of this work, however, is not to provide profile results and determine whether they are intuitively correct, but to provide quantitative thickness results for development of an efficient numerical code, which can then be used to investigate the parameter effects. Experimentally, it was impossible to change one parameter while holding the other parameters completely constant. This code can also provide more quantitative information on BLRO flow, such as the magnitude of temperature versus concentration-induced surface-tension gradients, the pressure and velocity distributions, and the relative magnitude of surface tension, gravity, and viscous effects. And, most importantly, this code can be used to screen and develop potential coating systems and BLRO solutions.

### References

- (1) Bauer, D.R. and Briggs, L.M., "Rheological Models for Predicting Flow in High Solids Coatings," *JOURNAL OF COATINGS TECHNOLOGY*, 56, No. 716, 87 (1984).
- (2) Pierce, P.E. and Schoff, C.K., *Coating Film Defects*, Federation Series on Coatings Technology, Federation of Societies for Coatings Technology, Philadelphia, PA, 7-25 (1988).
- (3) Blunk, R.H.J., "Surface-Tension-Driven Flows of Coatings: Bondline Readout Formation," Doctoral Dissertation, University of Michigan, 1996.
- (4) Fink-Jensen, P., "Surface Disturbances in Fluid Paint Films," *Farg och Lack*, 8, 5-14 (1962).
- (5) Nix, W.D., "Mechanical Properties of Thin Films," *Metall. Trans. A*, 20A, 2217-2245 (1989).
- (6) Schlichting, H., *Boundary Layer Theory*, 7th ed., McGraw-Hill Book Company, New York, 1979.
- (7) Marangoni, C.G.M., *Ann. Phys.*, 143, 337 (1872).
- (8) Holman, J.P., *Heat Transfer*, 6th ed., McGraw-Hill Book Company, New York, 1986.